Measurement-Induced Phase Transition for Free Fermions above One Dimension

Igor Poboiko, Igor V. Gornyi, and Alexander D. Mirlin
Institute for Quantum Materials and Technologies, Karlsruhe Institute of Technology, 76131 Karlsruhe, Germany
and Institut für Theorie der Kondensierten Materie, Karlsruhe Institute of Technology, 76131 Karlsruhe, Germany

A theory of the measurement-induced entanglement phase transition for free-fermion models in $d > 1$ dimensions is developed. The critical point separates a gapless phase with $\ell^{d-1}\ln\ell$ scaling of the second cumulant of the particle number and of the entanglement entropy and an area-law phase with ℓ^{d-1} scaling, where ℓ is a size of the subsystem. The problem is mapped onto an SU(R) replica nonlinear sigma model in $d+1$ dimensions, with $R \to 1$. Using renormalization-group analysis, we calculate critical indices in one-loop approximation justified for $d = 1+\epsilon$ with $\epsilon \ll 1$. Further, we carry out a numerical study of the transition for a $d = 2$ model on a square lattice, determine numerically the critical point, and estimate the critical index of the correlation length, $\nu \approx 1.4$.

Introduction.—Quantum dynamics of many-body systems subjected to quantum measurements and, in particular, measurement-induced entanglement phase transitions attract a great deal of research attention. This area of research connects the condensed matter physics with quantum information processing. Measurement-induced transitions, which result from a competition between unitary dynamics that enhances the entanglement and measurements that reduce it, were initially investigated in quantum-circuit framework [1–28]. Later works showed ubiquity of measurement-induced transitions; they were studied in a variety of many-body systems, including free fermions [29–45], Majorana fermions [46–48], Ising spin systems [49–58], Bose-Hubbard models [59–63], disordered systems with Anderson or many-body localization [38,64,65], and models of Sachdev-Ye-Kitaev type [66,67]. While most of the studies were of computational character, important analytical progress has been achieved for some of the models. Furthermore, recent works on trapped-ion systems [68,69] and superconducting quantum processors [70,71] reported experimental indications of measurement-induced phase transitions.

Recently, the present authors developed a field-theoretical approach to the measurement-induced physics in the model of one-dimensional free fermions [45]. The problem was mapped onto a two-dimensional SU(R) nonlinear sigma model (NLSM) in the replica limit $R \to 1$ blue; see also Refs. [27,46] for related NLSMs of different symmetries in Majorana fermion setups. The mapping to SU(R) NLSM allowed us to show that this system is always in the area-law phase but, for small measurement rate, exhibits a broad intermediate regime with logarithmic increase of the entropy. These analytical results were supported by numerical simulations.

In this Letter, we demonstrate that, in spatial dimensionality $d > 1$, the system of free fermions subjected to measurements exhibits a phase transition between a gapless phase with $\ell^{d-1}\ln\ell$ scaling of the second cumulant of the particle number and of the entanglement entropy and an area-law phase with ℓ^{d-1} scaling. (Here, ℓ is a size of the subsystem.) Specifically, on the analytical side, we map the problem onto a replica NLSM in $d+1$ dimensions and develop a renormalization group (RG) analysis. We show that for $d > 1$ and sufficiently rare measurements the scaling $\sim\ell^{d-1}\ln\ell$ holds. For $d = 1+\epsilon$ with $\epsilon \ll 1$ we develop a parametrically justified one-loop analysis of the transition and calculate critical indices. We identify the particle number covariance, closely related to the mutual information, as the scaling variable for the transition. Using this framework, we carry out a computational study of the transition in $d = 2$ dimensions, determine numerically the critical point, and estimate the correlation-length critical exponent ν. These arguments, together with the expectation of the quantum Zeno effect for sufficiently frequent measurements, imply the existence of the transition for arbitrary $d > 1$.

Model and measurement protocol.—We consider a d-dimensional tight-binding model of free fermions, defined on a hypercubic lattice with L^d sites and periodic boundary conditions. The system Hamiltonian reads

$$\hat{H} = -J\sum_{\langle \boldsymbol{x}\boldsymbol{x}'\rangle}\left[\hat{\psi}^\dagger(\boldsymbol{x})\hat{\psi}(\boldsymbol{x}') + \text{H.c.}\right], \tag{1}$$

where summation is performed over lattice links and the hopping constant J defines the energy scale. Each site $\boldsymbol{x}$ of the system is projectively monitored: at randomly chosen times $t_i^{(\boldsymbol{x})}$ sampled from a Poissonian distribution with a rate

γ, independently for each site, a projective measurement of the site occupation number $\hat{n}(\boldsymbol{x}) = \hat{\psi}^\dagger(\boldsymbol{x})\hat{\psi}(\boldsymbol{x})$ is performed. The outcome of such measurements, which can be either zero or unity, $n = 0, 1$, is random, with probabilities determined by the many-body wave function Ψ at time $t - 0$:

$$\mathrm{Prob}[n|(\boldsymbol{x}, t)] = \langle \Psi(t-0)|\hat{\mathbb{P}}_n(\boldsymbol{x})|\Psi(t-0)\rangle. \tag{2}$$

This standard quantum-mechanical Born rule involves many-body projectors onto linear subspaces with a definite site occupation $n = 0, 1$:

$$\hat{\mathbb{P}}_0(\boldsymbol{x}) = 1 - \hat{n}(\boldsymbol{x}), \qquad \hat{\mathbb{P}}_1(\boldsymbol{x}) = \hat{n}(\boldsymbol{x}). \tag{3}$$

After the measurement at time t on site $\boldsymbol{x}$ with an outcome n is performed, the wave function undergoes a von Neumann collapse and is projected onto the corresponding subspace with subsequent renormalization:

$$|\Psi(t+0)\rangle = \frac{\hat{\mathbb{P}}_n(\boldsymbol{x})|\Psi(t-0)\rangle}{\left\|\hat{\mathbb{P}}_n(\boldsymbol{x})|\Psi(t-0)\rangle\right\|}. \tag{4}$$

The system is initially prepared in an arbitrary Gaussian pure state (i.e., described by a Slater determinant) $|\Psi(t_0)\rangle$. The evolution consists of unitary part governed by the Hamiltonian $\hat{H}$ and nonunitary part introduced by measurements according to the above protocol. We will study properties of the wave function $|\Psi(t = 0)\rangle$ in the limit $t_0 \to -\infty$ ("steady state"). This pure state depends, by construction, on the random "measurement trajectory" $\mathcal{T} = \{t_m, \boldsymbol{x}_m, n_m\}$.

To investigate the measurement-induced entanglement transition, we utilize a relation [72] between the entanglement entropy $\mathcal{S}_E$ for a given subsystem A (characterized by the reduced density matrix $\hat{\rho}_A$) and an infinite series of particle-number cumulants,

$$\mathcal{C}_A^{(N)} = \langle\!\langle \left(\sum\nolimits_{\boldsymbol{x}\in A} \hat{n}(\boldsymbol{x})\right)^N \rangle\!\rangle, \tag{5}$$

in the same subsystem. This relation,

$$\mathcal{S}_E \equiv -\mathrm{Tr}(\hat{\rho}_A \ln \hat{\rho}_A) = \sum_{q=1}^{\infty} 2\zeta(2q)\mathcal{C}_A^{(2q)} \tag{6}$$

with ζ the zeta function, holds for arbitrary pure Gaussian states, including [38,43,45] monitored systems. Moreover, it was demonstrated [45] that the first term [involving the second particle-number cumulant $\mathcal{C}_A^{(2)}$] is dominant in the series (6), i.e., $\mathcal{S}_E \approx (\pi^2/3)\mathcal{C}_A^{(2)}$. This approximation is parametrically controlled for small measurement rate γ/J and holds numerically with an excellent precision even when γ/J is not small. We have verified that this is the case also for $d = 2$ across the transition [73]. This property is also known to hold in disordered systems [78], even in the vicinity of the Anderson metal-insulator transition. Notably, the present problem bears a certain similarity to that of Anderson transitions [79], as both can be mapped to corresponding NLSMs, albeit with different replica limits. For these reasons, our further analysis focuses on the second particle-number cumulant $\mathcal{C}_A^{(2)}$, with the results applying also to the entanglement entropy $\mathcal{S}_E$. Note that, in interacting systems, the above relation between $\mathcal{S}_E$ and particle-number fluctuations does not hold, making it possible to have a transition in particle-number fluctuations ("charge sharpening") distinct from the entanglement transition [25,26,69].

Nonlinear sigma model.—In Ref. [45], it was shown that the behavior of the particle-number cumulants (and of the entanglement entropy) in monitored one-dimensional free-fermion systems is described by a replicated NLSM. Specifically, this field theory operates with matrix fields $\hat{U}(\boldsymbol{x}, t) \in \mathrm{SU}(R)$ in the replica space, governed by the Lagrangian density

$$\mathcal{L}[\hat{U}] = \frac{g}{2}\mathrm{Tr}\left(\frac{1}{v_0}\partial_t^{\Xi}\hat{U}(\partial_t^{\Xi}\hat{U})^\dagger + v_0\nabla\hat{U}\nabla\hat{U}^\dagger\right), \tag{7}$$

and yields the observable correlation functions in the replica limit $R \to 1$ (dictated by the Born rule). The derivation of the effective theory (7) is straightforwardly extended to arbitrary spatial dimensionality d; as a result, we obtain the NLSM in $d + 1$ dimensions [73]. The theory is defined in the time domain $t \le 0$, with the boundary condition $\hat{U}(\boldsymbol{x}, t = 0) = \hat{\mathbb{I}}$. As a consequence of the measurement-induced infinite-temperature heating of the system in the steady state, velocity in Eq. (7) is expressed via the root-mean-square velocity averaged over the Brillouin zone $v = \sqrt{2d}J$ as $v_0 = v/\sqrt{d}$. The bare value of the coupling constant g is given by

$$g_0 = \rho(1-\rho)v_0/\gamma, \tag{8}$$

with $\rho \in [0, 1]$ being an average filling factor of the state (which is conserved during the evolution). The time derivative in Eq. (7) contains a source matrix field $\hat{\Xi}(\boldsymbol{x}, t)$, which is diagonal with respect to replica indices, $\hat{\Xi} = \mathrm{diag}(\{\Xi_r\}_{r=1}^R)$:

$$\partial_t^{\Xi}\hat{U} \equiv \partial_t\hat{U} + (iZ/2)\{\hat{U}, \hat{\Xi}\}. \tag{9}$$

Here, $\{.,.\}$ is the anticommutator and we have also introduced a renormalization factor Z with the bare value $Z_0 = 1$.

The generating functional $\mathcal{Z}[\hat{\Xi}]$ obtained from Eq. (7) in the presence of the source is then used to calculate the density correlation function that determines the

particle-number cumulants in Eq. (6). The simplest, two-point correlation function is given by

$$C(\boldsymbol{x}) = \overline{\langle\{\hat{n}(\boldsymbol{x}),\hat{n}(0)\}/2\rangle} - \overline{\langle\hat{n}(\boldsymbol{x})\rangle\langle\hat{n}(0)\rangle}$$
$$= -\lim_{\substack{t,t'\to 0\\ R\to 1}} \frac{1}{R-1}\left[\frac{g_0}{v_0}\delta(\boldsymbol{x})\delta(t-t') + \sum_{r=1}^{R}\frac{\delta^2 \ln \mathcal{Z}[\hat{\Xi}]}{\delta\Xi_r(\boldsymbol{x},t)\delta\Xi_r(0,t')}\right], \tag{10}$$

where the overbar denotes averaging over quantum trajectories $\mathcal{T}$. On the Gaussian level (i.e., expanding the fields in small fluctuations around the saddle point up to second order), this correlation function and its Fourier transform read

$$C(\boldsymbol{x}) = -2g_0 Z_0^2/\sigma_d|\boldsymbol{x}|^{d+1}, \qquad C(\boldsymbol{q}) = g_0 Z_0^2|\boldsymbol{q}|, \tag{11}$$

where $\sigma_d = 2\pi^{(d+1)/2}/\Gamma(d/2+1/2)$ is the surface area of d-dimensional sphere (with Γ the gamma function). For a subsystem in the form of a (d-dimensional) ball of radius ℓ, this correlation function leads to the following behavior of the second cumulant in the Gaussian approximation:

$$\mathcal{C}_\ell^{(2)} \simeq \frac{g_0}{\pi}\sigma_{d-1}\ell^{d-1}\ln\frac{\ell}{l_0}, \tag{12}$$

where $l_0 \simeq \sqrt{d/2}(J/\gamma)$ is the mean free path that plays a role of the ultraviolet cutoff for the NLSM. Importantly, a power-law ("critical") character (11) of $C(\boldsymbol{x})$ leads to a logarithmic enhancement of $\mathcal{C}_\ell^{(2)}$ and of the entanglement entropy in comparison to area law.

RG and scaling analysis.—The long-wavelength behavior of the NLSM (7) can be analyzed by means of RG equations for two running dimensionless coupling constants, $G(\ell) = g(\ell)\ell^{d-1}$ and $Z(\ell)$, cf. Refs. [80,81]. Since $d=1$ corresponds to the logarithmic dimension for the NLSM theory, we can develop an ϵ expansion with $\epsilon = d-1$. In the one-loop approximation, the RG flow is described by (cf. Ref. [45] where $\epsilon = 0$; see also [73])

$$dG/d\ln\ell \equiv \beta(G) = \epsilon G - R/4\pi + O(1/G), \tag{13}$$

$$d\ln Z/d\ln\ell \equiv \beta_Z(G) = O(1/G^2). \tag{14}$$

Equation (13) agrees with earlier results for the β function of the NLSM of corresponding symmetry [74,79–81].

For spatial dimensions higher than unity, $\epsilon > 0$, Eq. (13) implies the existence of a critical point defined by the condition $\beta(G_c) = 0$. Following an analogy with the Anderson metal-insulator transition, we will call the phase governed by an infrared-stable fixed point $G = 0$ "insulating," which corresponds to the area-law phase in the context of measurement-induced phase transitions. The phase with $G \to \infty$ will be referred to as "metallic," where the scaling of the cumulant with ℓ will be given by Eq. (12) with a renormalized prefactor. In the replica limit $R \to 1$ and to leading order in $\epsilon \ll 1$, we find the critical point separating these two phases at

$$G_c \approx 1/4\pi\epsilon + O(\epsilon^0), \tag{15}$$

akin to the critical conductance in Anderson transitions [79,82–85].

Expanding RG equations (13) and (14) around the critical point, $\beta(G) \approx \beta'(G_c)(G-G_c) \equiv (G-G_c)/\nu$ and $\beta_Z(G) \approx \beta_Z(G_c) \equiv \zeta/2$, we obtain the following one-loop results for the corresponding critical exponents:

$$\nu = 1/\epsilon + O(\epsilon^0), \qquad \zeta = 0 + O(\epsilon^2). \tag{16}$$

Integration of the RG equations in the vicinity of the critical point yields:

$$G(\ell) - G_c \approx (G_0 - G_c)\,(\ell/l_0)^{1/\nu}, \qquad Z(\ell) \approx (\ell/l_0)^{\zeta/2}. \tag{17}$$

The length scale at which $|G - G_c| \sim G_c$ defines the correlation length

$$l_{\mathrm{corr}} \sim l_0(|G_0 - G_c|/G_c)^{-\nu}. \tag{18}$$

We study now the behavior of the renormalized density correlation function $C(r)$, Eq. (10), considering first the critical point, $G_0 \equiv G(l_0) = G_c$. Performing the RG transformation up to the scale r and then evaluating the Gaussian integral as in Eq. (11), we obtain

$$C(r) \sim -g(r)Z^2(r)r^{-d-1} \sim -G_c r^{-2d}(r/l_0)^\zeta. \tag{19}$$

According to Eq. (10), $C(\boldsymbol{x}-\boldsymbol{x}')$ at $\boldsymbol{x} \neq \boldsymbol{x}'$ is a correlation function of Noether currents $\hat{\mathcal{J}}_t = (-i/2)(\hat{U}^\dagger\partial_t\hat{U} - \hat{U}\partial_t\hat{U}^\dagger)$ at $\boldsymbol{x}$ and $\boldsymbol{x}'$. It is known that surface integrals of conserved currents are symmetry generators [86] and thus have scaling dimension zero at criticality [87,88]. Thus, our currents $\hat{\mathcal{J}}_t$ should have scaling dimension d, implying that $C(\boldsymbol{x}-\boldsymbol{x}') \propto |\boldsymbol{x}-\boldsymbol{x}'|^{-2d}$ and hence $\zeta = 0$.

Extending this analysis to G_0 around G_c, we get

$$C(r) \simeq -\frac{G(r)}{r^{2d}} = -\frac{G_c}{r^{2d}} f\left(\frac{r}{l_{\mathrm{corr}}}\right), \tag{20}$$

where $f(x)$ is a universal scaling function with two branches describing both sides of the transition. The $x \ll 1$ behavior of $f(x)$ describes the critical point and its vicinity. According to Eq. (17), we have

$$f(x \ll 1) \approx \begin{cases} 1 + x^{1/\nu}, & G_0 > G_c, \\ 1 - x^{1/\nu}, & G_0 < G_c. \end{cases} \tag{21}$$

The $x \gg 1$ behavior of $f(x)$ corresponds to the "metallic" and "insulating" phases. On the "metallic" side of the transition, Eq. (20) should reproduce the asymptotics $C(r) \propto -1/r^{d+1}$. In the area-law phase, one expects $C(r)$ to decay exponentially fast at infinity. To match this asymptotic behavior, the scaling function should satisfy

$$f(x \gg 1) \sim \begin{cases} x^{d-1}, & G_0 > G_c, \\ e^{-x}, & G_0 < G_c. \end{cases} \tag{22}$$

It is worth emphasizing that the derivation of the NLSM and its RG analysis are under full control for $G \gg 1$. Thus, the analytical treatment of the transition is parametrically controllable at $\epsilon \ll 1$, when $G_c \gg 1$. At the same time, physically more interesting dimensions d are integer, such as $d = 2$ or $d = 3$. On general grounds, we expect that the above scaling analysis also applies to $d = 2, 3$, in similarity to ϵ expansions for Anderson transitions and statistical-mechanics transitions. Below, we study numerically the $d = 2$ model to verify these scaling predictions and to estimate the critical exponent ν.

Particle number covariance and mutual information.—According to the above analysis, $\mathcal{C}_A^{(2)}$ and $\mathcal{S}_E$ scale as $\ell^{d-1} \ln \ell$ in the "metallic" phase and exhibit the area-law scaling both in the "insulating" phase and at criticality. In order to locate the transition and to probe the scaling around it, it is advantageous to consider an observable with three distinct forms of scaling, in analogy with the conductance around the Anderson transition. With this motivation, we analyze the particle-number covariance of two regions, A and B,

$$\overline{G_{AB}} = -\overline{\langle\langle \hat{N}_A \hat{N}_B \rangle\rangle} = -\int_A d^d\boldsymbol{x} \int_B d^d\boldsymbol{y} C(\boldsymbol{x}-\boldsymbol{y}). \tag{23}$$

If both regions have characteristic size $\ell_A, \ell_B \sim \ell$, and the separation between those regions is also of the same order, the scaling of G_{AB} should read, according to Eqs. (20)–(22),

$$\overline{G_{AB}} \simeq \tilde{f}(\ell/l_{\rm corr}) \sim \begin{cases} c_1(\ell/l_{\rm corr})^{d-1}, & G_0 > G_c, \\ c_2 G_c, & G_0 = G_c, \\ \exp(-c_3 \ell/l_{\rm corr}), & G_0 < G_c, \end{cases} \tag{24}$$

with numerical factors $c_{1,2,3} = O(1)$ depending on the exact geometry under consideration. Since $C(\boldsymbol{x}-\boldsymbol{y})$ is a correlation function of Noether currents, $-C(\boldsymbol{x}-\boldsymbol{y})$ has a meaning of two-point conductance within the Anderson-transition analogy, and G_{AB} has the meaning of conductance of a system with two leads attached to regions A and B. Furthermore, G_{AB} can be related to the mutual information $I(A:B)$ between these regions,

$$I(A:B) = \mathcal{S}_E(A) + \mathcal{S}_E(B) - \mathcal{S}_E(A \cup B) \simeq \frac{2\pi^2}{3} G_{AB}, \tag{25}$$

implying that $I(A:B)$ exhibits the same scaling (24). Thus, it can also be used as a probe of the transition.

Numerical analysis.—To verify and complement our analytical theory, we carried out direct numerical simulations of dynamics of a monitored two-dimensional free-fermion system following the protocol outlined above. As the protocol preserves the Gaussian nature of the state, the system is fully characterized by the single-particle Green function $\mathcal{G}_{\boldsymbol{x}\boldsymbol{x}'} \equiv \langle \hat{\psi}^\dagger(\boldsymbol{x}) \hat{\psi}(\boldsymbol{x}') \rangle$. Executing unitary evolution along with projective measurements until the system has reached the steady state, we evaluated the two-point density correlation function on a lattice:

$$C_{\boldsymbol{x}\boldsymbol{x}'} = \langle \hat{n}(\boldsymbol{x}) \hat{n}(\boldsymbol{x}') \rangle - \langle \hat{n}(\boldsymbol{x}) \rangle \langle \hat{n}(\boldsymbol{x}') \rangle = \mathcal{G}_{\boldsymbol{x}\boldsymbol{x}} \delta_{\boldsymbol{x}\boldsymbol{x}'} - \mathcal{G}_{\boldsymbol{x}\boldsymbol{x}'} \mathcal{G}_{\boldsymbol{x}'\boldsymbol{x}}. \tag{26}$$

The protocol was repeated ∼100 times, and averaging over quantum trajectories and over positions in the sample was performed to calculate $C(\boldsymbol{x}-\boldsymbol{x}') = \overline{C_{\boldsymbol{x}\boldsymbol{x}'}}$.

The results obtained for an $L \times L$ system with periodic boundary conditions and $L = 40$ are shown in Fig. 1. According to the above analytical discussion, the transition can be characterized by the behavior of $\lim_{q\to 0} C(q)/q$, which is expected to be finite in the "metallic" phase and zero in the "insulating" phase [where $C(q) \propto q^2$ due to exponential decay of $C(r)$]. The $q \to 0$ values extrapolated from the finite-size curves (see inset) are fully consistent

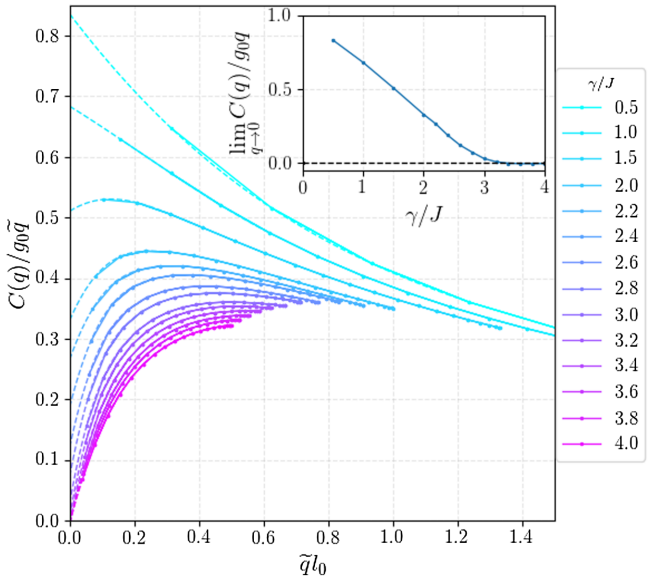

FIG. 1. Correlation function $C(q)$ of an $L \times L$ system with $L = 40$ across the transition. Shown are dependencies of $C(q)/g_0\tilde{q}$ on $\tilde{q}l_0$ [with $\tilde{q} = 2\sin(q/2)$] for values of the measurement rate γ/J from 0.5 to 4.0. Dashed lines: cubic polynomial extrapolation down to $q \to 0$ using five lowest momenta. Inset: the extrapolated value at $q \to 0$ as a function of γ/J. For $\gamma > \gamma_c$, where $\gamma_c/J \simeq 3.2$, the extrapolated value is zero within numerical precision, which is a manifestation of the measurement-induced phase transition.

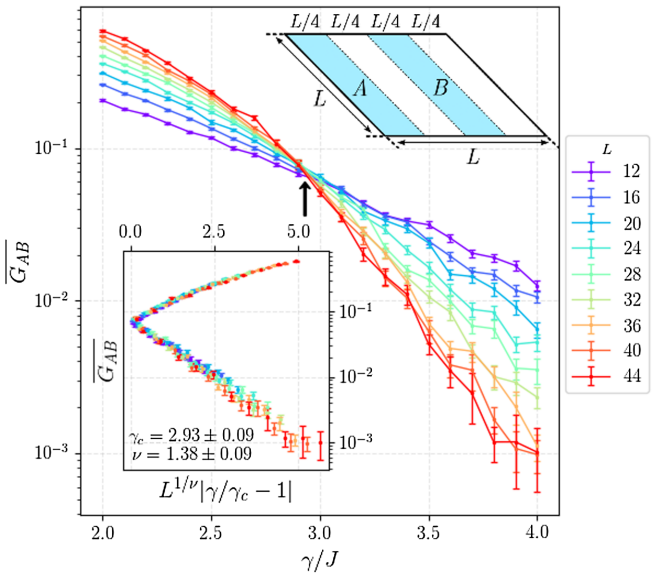

FIG. 2. Particle number covariance $\overline{G_{AB}}$ between two regions A and B in a geometrical setup shown in upper inset, as a function of ratio γ/J for different system sizes L. Arrow marks the estimated position of the transition, manifesting itself as a crossing point of all curves,; see Eq. (24). Inset: collapse according to Eq. (24) with a scaling function $\tilde{f}(x^\nu)$, where x is given by the expression labeling the x axis of the inset. Obtained values of γ_c and ν are shown.

with this prediction, yielding an estimate $\gamma_c/J \approx 3.2$ for the critical point. Furthermore, at $\gamma \to 0$, the Gaussian approximation (11) is parametrically justified and predicts that $C(q)/g_0 q$ should saturate at unity, which is also in excellent agreement with the numerical data. For more details of numerical analysis of $C(q)$, see Ref. [73].

To explore the transition more accurately, we focus now on the scaling of the particle number covariance (23) in a narrower vicinity of the transition point γ_c. We use a geometrical setup consisting of two regions of size $L/4 \times L$ separated by distance $L/4$, see upper inset of Fig. 2. According to Eqs. (18) and (24), the data for $\overline{G_{AB}}$ should collapse, with a suitable choice of γ_c and critical exponent ν, on a single universal function $\tilde{f}(x)$. Figure 2 demonstrates the behavior of $\overline{G_{AB}}$ as a function of γ for system sizes from $L = 12$ to $L = 44$. A well-pronounced crossing point of all curves is observed, providing a more accurate value for the transition point, $\gamma_c/J \approx 2.9 \pm 0.1$. As shown in the lower inset, a good scaling collapse can be achieved, yielding the critical exponent $\nu = 1.4 \pm 0.1$. More general collapse of the form $\overline{G_{AB}}/L^\zeta = \tilde{f}(L/\ell_{\rm corr})$, which keeps the value of the critical exponent ζ finite, yields an indistinguishable from zero value $\zeta \sim 10^{-4}$, confirming our analytical prediction $\zeta = 0$. Collapse analysis was performed using PYFSSA package [73,89,90], which yields γ_c and ν with error bars.

Summary.—We have developed a field theory for monitored d-dimensional free-fermion systems, which has a form of an SU(R) NLSM in $d+1$ dimensions, with the $R \to 1$ replica limit. By performing its RG analysis, we have demonstrated the existence of a measurement-induced entanglement phase transition in such models for dimensions $d > 1$. The transition point separates a symmetry-broken "metallic" phase realized for rare measurements and characterized by $\ell^{d-1} \ln \ell$ scaling of the second particle-number cumulant and the entanglement entropy from the "insulating" area-law phase for frequent measurements. We have further calculated critical indices in the one-loop order of ϵ expansion in $d = 1 + \epsilon$ dimensions. Additionally, numerical investigation of the $d = 2$ model on a square lattice enabled us to pinpoint the critical point and to estimate the correlation-length exponent $\nu = 1.4 \pm 0.1$. The measurement-induced entanglement transition for free fermions in dimensions $d > 1$ bears a striking similarity to Anderson metal-insulator transition in disordered systems of $d+1$ dimensions. In the present context, it is the quantum information (closely related to particle-number fluctuations) that experiences localization. As future important generalizations of the theory, we envisage inclusion of interaction and/or of static disorder, as well as measurement protocols generating nontrivial topology.

Note added.—We have learned about a parallel related activity by K. Chahine and M. Buchhold [91]. After submission of our paper, a preprint [92] appeared, which reports a transition for a $d > 2$ *single-particle* continuously monitored problem.

We are grateful to A. Altland, D. Bernard, M. Buchhold, K. Chahine, S. Diehl, E. Doggen, Y. Gefen, I. Gruzberg, P. Ostrovsky, P. Pöpperl, M. Szyniszewski, and R. Vasseur for fruitful discussions. We acknowledge support by the Deutsche Forschungsgemeinschaft (DFG) via the Grants No. MI 658/14-1 and No. GO 1405/6-1.

[1] Y. Li, X. Chen, and M. P. A. Fisher, Quantum Zeno effect and the many-body entanglement transition, Phys. Rev. B **98**, 205136 (2018).
[2] B. Skinner, J. Ruhman, and A. Nahum, Measurement-induced phase transitions in the dynamics of entanglement, Phys. Rev. X **9**, 031009 (2019).
[3] A. Chan, R. M. Nandkishore, M. Pretko, and G. Smith, Unitary-projective entanglement dynamics, Phys. Rev. B **99**, 224307 (2019).
[4] M. Szyniszewski, A. Romito, and H. Schomerus, Entanglement transition from variable-strength weak measurements, Phys. Rev. B **100**, 064204 (2019).
[5] Y. Li, X. Chen, and M. P. A. Fisher, Measurement-driven entanglement transition in hybrid quantum circuits, Phys. Rev. B **100**, 134306 (2019).
[6] Y. Bao, S. Choi, and E. Altman, Theory of the phase transition in random unitary circuits with measurements, Phys. Rev. B **101**, 104301 (2020).

[7] S. Choi, Y. Bao, X.-L. Qi, and E. Altman, Quantum error correction in scrambling dynamics and measurement-induced phase transition, Phys. Rev. Lett. **125**, 030505 (2020).

[8] M. J. Gullans and D. A. Huse, Dynamical purification phase transition induced by quantum measurements, Phys. Rev. X **10**, 041020 (2020).

[9] M. J. Gullans and D. A. Huse, Scalable probes of measurement-induced criticality, Phys. Rev. Lett. **125**, 070606 (2020).

[10] C.-M. Jian, Y.-Z. You, R. Vasseur, and A. W. W. Ludwig, Measurement-induced criticality in random quantum circuits, Phys. Rev. B **101**, 104302 (2020).

[11] A. Zabalo, M. J. Gullans, J. H. Wilson, S. Gopalakrishnan, D. A. Huse, and J. H. Pixley, Critical properties of the measurement-induced transition in random quantum circuits, Phys. Rev. B **101**, 060301(R) (2020).

[12] J. Iaconis, A. Lucas, and X. Chen, Measurement-induced phase transitions in quantum automaton circuits, Phys. Rev. B **102**, 224311 (2020).

[13] X. Turkeshi, R. Fazio, and M. Dalmonte, Measurement-induced criticality in $(2+1)$-dimensional hybrid quantum circuits, Phys. Rev. B **102**, 014315 (2020).

[14] L. Zhang, J. A. Reyes, S. Kourtis, C. Chamon, E. R. Mucciolo, and A. E. Ruckenstein, Nonuniversal entanglement level statistics in projection-driven quantum circuits, Phys. Rev. B **101**, 235104 (2020).

[15] M. Szyniszewski, A. Romito, and H. Schomerus, Universality of entanglement transitions from stroboscopic to continuous measurements, Phys. Rev. Lett. **125**, 210602 (2020).

[16] A. Nahum, S. Roy, B. Skinner, and J. Ruhman, Measurement and entanglement phase transitions in all-to-all quantum circuits, on quantum trees, and in Landau-Ginsburg theory, PRX Quantum **2**, 010352 (2021).

[17] M. Ippoliti, M. J. Gullans, S. Gopalakrishnan, D. A. Huse, and V. Khemani, Entanglement phase transitions in measurement-only dynamics, Phys. Rev. X **11**, 011030 (2021).

[18] M. Ippoliti and V. Khemani, Postselection-free entanglement dynamics via spacetime duality, Phys. Rev. Lett. **126**, 060501 (2021).

[19] A. Lavasani, Y. Alavirad, and M. Barkeshli, Measurement-induced topological entanglement transitions in symmetric random quantum circuits, Nat. Phys. **17**, 342 (2021).

[20] A. Lavasani, Y. Alavirad, and M. Barkeshli, Topological order and criticality in $(2+1)$D monitored random quantum circuits, Phys. Rev. Lett. **127**, 235701 (2021).

[21] S. Sang and T. H. Hsieh, Measurement-protected quantum phases, Phys. Rev. Res. **3**, 023200 (2021).

[22] M. P. Fisher, V. Khemani, A. Nahum, and S. Vijay, Random quantum circuits, Annu. Rev. Condens. Matter Phys. **14**, 335 (2023).

[23] M. Block, Y. Bao, S. Choi, E. Altman, and N. Y. Yao, Measurement-induced transition in long-range interacting quantum circuits, Phys. Rev. Lett. **128**, 010604 (2022).

[24] S. Sharma, X. Turkeshi, R. Fazio, and M. Dalmonte, Measurement-induced criticality in extended and long-range unitary circuits, SciPost Phys. Core **5**, 023 (2022).

[25] U. Agrawal, A. Zabalo, K. Chen, J. H. Wilson, A. C. Potter, J. H. Pixley, S. Gopalakrishnan, and R. Vasseur, Entanglement and charge-sharpening transitions in U(1) symmetric monitored quantum circuits, Phys. Rev. X **12**, 041002 (2022).

[26] F. Barratt, U. Agrawal, S. Gopalakrishnan, D. A. Huse, R. Vasseur, and A. C. Potter, Field theory of charge sharpening in symmetric monitored quantum circuits, Phys. Rev. Lett. **129**, 120604 (2022).

[27] C.-M. Jian, H. Shapourian, B. Bauer, and A. W. W. Ludwig, Measurement-induced entanglement transitions in quantum circuits of non-interacting fermions: Born-rule versus forced measurements, arXiv:2302.09094.

[28] S. P. Kelly, U. Poschinger, F. Schmidt-Kaler, M. P. A. Fisher, and J. Marino, Coherence requirements for quantum communication from hybrid circuit dynamics, SciPost Phys. **15**, 250 (2023).

[29] X. Cao, A. Tilloy, and A. De Luca, Entanglement in a fermion chain under continuous monitoring, SciPost Phys. **7**, 024 (2019).

[30] O. Alberton, M. Buchhold, and S. Diehl, Entanglement transition in a monitored free-fermion chain: From extended criticality to area law, Phys. Rev. Lett. **126**, 170602 (2021).

[31] X. Chen, Y. Li, M. P. A. Fisher, and A. Lucas, Emergent conformal symmetry in nonunitary random dynamics of free fermions, Phys. Rev. Res. **2**, 033017 (2020).

[32] Q. Tang, X. Chen, and W. Zhu, Quantum criticality in the nonunitary dynamics of $(2+1)$-dimensional free fermions, Phys. Rev. B **103**, 174303 (2021).

[33] M. Coppola, E. Tirrito, D. Karevski, and M. Collura, Growth of entanglement entropy under local projective measurements, Phys. Rev. B **105**, 094303 (2022).

[34] B. Ladewig, S. Diehl, and M. Buchhold, Monitored open fermion dynamics: Exploring the interplay of measurement, decoherence, and free Hamiltonian evolution, Phys. Rev. Res. **4**, 033001 (2022).

[35] F. Carollo and V. Alba, Entangled multiplets and spreading of quantum correlations in a continuously monitored tight-binding chain, Phys. Rev. B **106**, L220304 (2022).

[36] M. Buchhold, T. Müller, and S. Diehl, Revealing measurement-induced phase transitions by pre-selection, arXiv:2208.10506.

[37] Q. Yang, Y. Zuo, and D. E. Liu, Keldysh nonlinear sigma model for a free-fermion gas under continuous measurements, Phys. Rev. Res. **5**, 033174 (2023).

[38] M. Szyniszewski, O. Lunt, and A. Pal, Disordered monitored free fermions, Phys. Rev. B **108**, 165126 (2023).

[39] M. Buchhold, Y. Minoguchi, A. Altland, and S. Diehl, Effective theory for the measurement-induced phase transition of Dirac fermions, Phys. Rev. X **11**, 041004 (2021).

[40] M. Van Regemortel, Z.-P. Cian, A. Seif, H. Dehghani, and M. Hafezi, Entanglement entropy scaling transition under competing monitoring protocols, Phys. Rev. Lett. **126**, 123604 (2021).

[41] Y. L. Gal, X. Turkeshi, and M. Schirò, Volume-to-area law entanglement transition in a non-Hermitian free fermionic chain, SciPost Phys. **14**, 138 (2023).

[42] H. Lóio, A. De Luca, J. De Nardis, and X. Turkeshi, Purification timescales in monitored fermions, Phys. Rev. B **108**, L020306 (2023).

[43] X. Turkeshi, L. Piroli, and M. Schiró, Enhanced entanglement negativity in boundary-driven monitored fermionic chains, Phys. Rev. B **106**, 024304 (2022).

[44] G. Kells, D. Meidan, and A. Romito, Topological transitions in weakly monitored free fermions, SciPost Phys. **14**, 031 (2023).

[45] I. Poboiko, P. Pöpperl, I. V. Gornyi, and A. D. Mirlin, Theory of free fermions under random projective measurements, Phys. Rev. X **13**, 041046 (2023).

[46] M. Fava, L. Piroli, T. Swann, D. Bernard, and A. Nahum, Nonlinear sigma models for monitored dynamics of free fermions, Phys. Rev. X **13**, 041045 (2023).

[47] T. Swann, D. Bernard, and A. Nahum, Spacetime picture for entanglement generation in noisy fermion chains, arXiv: 2302.12212.

[48] J. Merritt and L. Fidkowski, Entanglement transitions with free fermions, Phys. Rev. B **107**, 064303 (2023).

[49] N. Lang and H. P. Büchler, Entanglement transition in the projective transverse field Ising model, Phys. Rev. B **102**, 094204 (2020).

[50] D. Rossini and E. Vicari, Measurement-induced dynamics of many-body systems at quantum criticality, Phys. Rev. B **102**, 035119 (2020).

[51] A. Biella and M. Schirò, Many-body quantum Zeno effect and measurement-induced subradiance transition, Quantum **5**, 528 (2021).

[52] X. Turkeshi, A. Biella, R. Fazio, M. Dalmonte, and M. Schirò, Measurement-induced entanglement transitions in the quantum Ising chain: From infinite to zero clicks, Phys. Rev. B **103**, 224210 (2021).

[53] E. Tirrito, A. Santini, R. Fazio, and M. Collura, Full counting statistics as probe of measurement-induced transitions in the quantum Ising chain, SciPost Phys. **15**, 096 (2023).

[54] Z. Yang, D. Mao, and C.-M. Jian, Entanglement in a one-dimensional critical state after measurements, Phys. Rev. B **108**, 165120 (2023).

[55] Z. Weinstein, R. Sajith, E. Altman, and S. J. Garratt, Nonlocality and entanglement in measured critical quantum Ising chains, Phys. Rev. B **107**, 245132 (2023).

[56] S. Murciano, P. Sala, Y. Liu, R. S. K. Mong, and J. Alicea, Measurement-altered Ising quantum criticality, Phys. Rev. X **13**, 041042 (2023).

[57] P. Sierant, G. Chiriacò, F. M. Surace, S. Sharma, X. Turkeshi, M. Dalmonte, R. Fazio, and G. Pagano, Dissipative Floquet dynamics: From steady state to measurement induced criticality in trapped-ion chains, Quantum **6**, 638 (2022).

[58] X. Turkeshi, M. Dalmonte, R. Fazio, and M. Schirò, Entanglement transitions from stochastic resetting of non-Hermitian quasiparticles, Phys. Rev. B **105**, L241114 (2022).

[59] Q. Tang and W. Zhu, Measurement-induced phase transition: A case study in the nonintegrable model by density-matrix renormalization group calculations, Phys. Rev. Res. **2**, 013022 (2020).

[60] S. Goto and I. Danshita, Measurement-induced transitions of the entanglement scaling law in ultracold gases with controllable dissipation, Phys. Rev. A **102**, 033316 (2020).

[61] Y. Fuji and Y. Ashida, Measurement-induced quantum criticality under continuous monitoring, Phys. Rev. B **102**, 054302 (2020).

[62] E. V. H. Doggen, Y. Gefen, I. V. Gornyi, A. D. Mirlin, and D. G. Polyakov, Generalized quantum measurements with matrix product states: Entanglement phase transition and clusterization, Phys. Rev. Res. **4**, 023146 (2022).

[63] E. V. H. Doggen, Y. Gefen, I. V. Gornyi, A. D. Mirlin, and D. G. Polyakov, Evolution of many-body systems under ancilla quantum measurements, Phys. Rev. B **107**, 214203 (2023).

[64] O. Lunt and A. Pal, Measurement-induced entanglement transitions in many-body localized systems, Phys. Rev. Res. **2**, 043072 (2020).

[65] K. Yamamoto and R. Hamazaki, Localization properties in disordered quantum many-body dynamics under continuous measurement, Phys. Rev. B **107**, L220201 (2023).

[66] S.-K. Jian, C. Liu, X. Chen, B. Swingle, and P. Zhang, Measurement-induced phase transition in the monitored Sachdev-Ye-Kitaev model, Phys. Rev. Lett. **127**, 140601 (2021).

[67] A. Altland, M. Buchhold, S. Diehl, and T. Micklitz, Dynamics of measured many-body quantum chaotic systems, Phys. Rev. Res. **4**, L022066 (2022).

[68] C. Noel, P. Niroula, D. Zhu, A. Risinger, L. Egan, D. Biswas, M. Cetina, A. V. Gorshkov, M. J. Gullans, D. A. Huse, and C. Monroe, Measurement-induced quantum phases realized in a trapped-ion quantum computer, Nat. Phys. **18**, 760 (2022).

[69] U. Agrawal, J. Lopez-Piqueres, R. Vasseur, S. Gopalakrishnan, and A. C. Potter, Observing quantum measurement collapse as a learnability phase transition, arXiv:2311.00058.

[70] J. M. Koh, S.-N. Sun, M. Motta, and A. J. Minnich, Measurement-induced entanglement phase transition on a superconducting quantum processor with mid-circuit readout, Nat. Phys. **19**, 1314 (2023).

[71] J. C. Hoke *et al.* (Google Quantum AI and Collaborators), Measurement-induced entanglement and teleportation on a noisy quantum processor, Nature (London) **622**, 481 (2023).

[72] I. Klich and L. Levitov, Quantum noise as an entanglement meter, Phys. Rev. Lett. **102**, 100502 (2009).

[73] See Supplemental Material at http://link.aps.org/supplemental/10.1103/PhysRevLett.132.110403, which includes details of the theoretical analysis and computational approach, and which includes Refs. [74–77].

[74] E. J. König, P. M. Ostrovsky, I. V. Protopopov, and A. D. Mirlin, Metal-insulator transition in two-dimensional random fermion systems of chiral symmetry classes, Phys. Rev. B **85**, 195130 (2012).

[75] J. A. Nelder and R. Mead, A simplex method for function minimization, Comput. J. **7**, 308 (1965).

[76] A. Sorge, PYFSSA Documentation: The quality of data collapse (2015).

[77] J. Houdayer and A. K. Hartmann, Low-temperature behavior of two-dimensional Gaussian Ising spin glasses, Phys. Rev. B **70**, 014418 (2004).

[78] I. Burmistrov, K. Tikhonov, I. Gornyi, and A. Mirlin, Entanglement entropy and particle number cumulants of disordered fermions, Ann. Phys. (N.Y.) **383**, 140 (2017).

[79] F. Evers and A. D. Mirlin, Anderson transitions, Rev. Mod. Phys. **80**, 1355 (2008).

[80] S. Hikami, Three-loop β-functions of non-linear σ models on symmetric spaces, Phys. Lett. **98B**, 208 (1981).
[81] F. Wegner, Four-loop-order β-function of nonlinear σ-models in symmetric spaces, Nucl. Phys. **B316**, 663 (1989).
[82] E. Abrahams, P. W. Anderson, D. C. Licciardello, and T. V. Ramakrishnan, Scaling theory of localization: Absence of quantum diffusion in two dimensions, Phys. Rev. Lett. **42**, 673 (1979).
[83] B. Kramer and A. MacKinnon, Localization: Theory and experiment, Rep. Prog. Phys. **56**, 1469 (1993).
[84] K. Slevin and T. Ohtsuki, The Anderson transition: Time reversal symmetry and universality, Phys. Rev. Lett. **78**, 4083 (1997).
[85] B. Shapiro, Conductance distribution at the mobility edge, Phys. Rev. Lett. **65**, 1510 (1990).
[86] P. Di Francesco, P. Mathieu, and D. Sénéchal, *Conformal Field Theory* (Springer, New York, 1997).
[87] D. J. Gross, Applications of the renormalization group to high-energy physics, in *Methods in Field Theory* (North-Holland Publishing Co., Amsterdam, 1976), pp. 141–250.
[88] X.-G. Wen, Scaling theory of conserved current and universal amplitudes at anisotropic critical points, Phys. Rev. B **46**, 2655 (1992).
[89] A. Sorge, PYFSSA 0.7.6 (2015).
[90] O. Melchert, autoscale.py—a program for automatic finite-size scaling analyses: A user's guide, arXiv:0910.5403.
[91] K. Chahine and M. Buchhold, Entanglement phases, localization and multifractality of monitored free fermions in two dimensions, arXiv:2309.12391.
[92] T. Jin and D. G. Martin, Measurement-induced phase transition in a single-body tight-binding model, arXiv:2309.15034.